International Journal of Hydrogen Energy 275 (2026) 157502

Contents lists available at ScienceDirect

International Journal of Hydrogen Energy

journal homepage: www.elsevier.com/locate/he

Polyoxymethylene ethers as attractive hydrogen transport vectors? - Concept evaluation and steam reforming investigations

Fabian Kroll [a], Michael Geißelbrecht [a], Patrick Schühle [b,c,*]

[a] Forschungszentrum Jülich GmbH, Helmholtz Institut Erlangen-Nürnberg for Renewable Energy (IET-2), Cauerstraße 1, Erlangen, 91058, Germany
[b] Lehrstuhl für Chemische Reaktionstechnik, Friedrich-Alexander-Universität Erlangen-Nürnberg, Egerlandstraße 3, Erlangen, 91058, Germany
[c] Forschungszentrum Jülich GmbH, Institute for a sustainable Hydrogen Economy (IHE-3), Wilhelm-Johnen-Straße, Jülich, DE-52428, Germany

ARTICLE INFO

Keywords:
Polyoxymethylene ether (OME)
Steam reforming
Hydrogen carrier
Indium oxide
OME/CO_2 transport cycle

ABSTRACT

The efficient and safe transportation of renewable hydrogen remains a major challenge. Polyoxymethylene dimethyl ethers (OMEs) might be promising hydrogen transport vectors due to their liquid state at ambient conditions, low toxicity and high technical hydrogen capacity. However, two major bottlenecks for their application are identified: the direct synthesis of OMEs from CO_2 and H_2 and the catalytic steam reforming of OMEs for hydrogen release, which remains largely unexplored. A hydrogen transport cycle based on OME_1 is proposed and compared with methanol and dimethyl ether regarding technical and energetic characteristics. Experimentally, OME_{1-3} steam reforming is investigated over In_2O_3/ZrO_2 catalysts. High OME conversion, hydrogen yield and long-term stability over 380 h on stream are achieved. OME hydrolysis is facilitated compared with dimethyl ether and requires no additional acidic catalyst. For the first time, OME_2 and OME_3 are successfully steam-reformed with comparable rates and stability to OME_1.

1. Introduction

According to the European Green Deal, the European Union aims to become the first climate-neutral continent by achieving net-zero greenhouse gas emissions by 2050 [1]. To meet this ambitious goal, Europe will depend heavily on imports of green hydrogen from regions with cheap and abundant renewable electricity [2]. For short transport distances (less than 100 km), pipelines offer the most efficient solution. However, for long-distance hydrogen transport, maritime shipping is the most viable option [3,4]. Transporting molecular hydrogen presents considerable challenges due to its low volumetric energy density and high boil-off losses [5]. An attractive alternative approach involves chemically binding hydrogen to carrier molecules, thereby minimizing losses during transport. In addition to well-studied hydrogen carriers such as ammonia, methanol, synthetic methane and liquid organic hydrogen carriers (LOHCs), recently dimethyl ether (DME) gained attention as a promising alternative for hydrogen storage and transport [6,7].

Our group has proposed a DME/CO_2 cycle for point-to-point hydrogen transport over long distances. The concept takes advantage of the similar physical properties of dimethyl ether (DME) and CO_2 to enable efficient back-shipping of CO_2 following hydrogen release from DME at the destination [8]. Fundamentally in this cycle, DME is synthesized (equation (1))) at renewable energy-rich locations using hydrogen from water electrolysis and CO_2, partially captured directly from the atmosphere and partially recycled from the back shipping. This process produces water as a byproduct, which can, in turn, be reused to support the electrolysis step, contributing to the overall sustainability of the cycle. Although commercial DME is currently produced either via methanol dehydration or direct synthesis from CO-containing syngas ($CO/CO_2/H_2$), alternative production routes based on renewable H_2 and captured or recycled CO_2 have reached an advanced stage of development [9].

$$2CO_2 + 6\,H_2 \rightleftharpoons CH_3OCH_3 + 3\,H_2O \quad (1)$$

DME offers the advantage of a high technical hydrogen capacity ($w_{H2,technical}$) of 26.1 wt%, enabling the provision of a large amount of hydrogen per unit carrier mass.

$$w_{H2,technical} = \frac{m_{H2,released}}{m_{Carrier}} \quad (2)$$

However, under ambient conditions, DME exists as a gas and must therefore be liquefied for volume efficient transportation. To prevent

* Corresponding author. Lehrstuhl für Chemische Reaktionstechnik, Friedrich-Alexander-Universität Erlangen-Nürnberg, Egerlandstraße 3, 91058, Erlangen, Germany
E-mail address: Patrick.schuehle@fau.de (P. Schühle).

https://doi.org/10.1016/j.ijhydene.2026.157502
Received 2 January 2026; Received in revised form 8 August 2026; Accepted 7 September 2026
Available online 18 September 2026
0360-3199/© 2026 The Authors. Published by Elsevier Ltd on behalf of Hydrogen Energy Publications LLC. This is an open access article under the CC BY-NC-ND license (http://creativecommons.org/licenses/by-nc-nd/4.0/).

Glossary

OME	polyoxymethylene dimethyl ethers
DME	Dimethyl ether
LOHC	Liquid organic hydrogen carriers
DMM/OME_1	Dimethoxymethane
MF	Methyl formate
FA	Formaldehyde
MM	Methoxy methanol
MeOH	Methanol
LCO_2	Liquefied CO_2
DAC	Direct air capture
WHSV	Weight hourly space velocity
rWGS	Reverse water-gas shift

excessive boil-off losses during transport, the liquid DME must be maintained at a constant low temperature of around −24 °C under ambient pressure or by combining slight overpressure and cooling. Compared to molecular hydrogen or synthetic methane, which require cryogenic conditions below −252 °C and −162 °C, respectively, DME offers a more manageable storage temperature and exhibits significantly lower boil-off losses of about 0.017 % d^{-1} [5]. DME also exhibits a lower global warming potential than methane or methanol [5].

At the transport destination, hydrogen is released via DME steam reforming (DME-SR, reverse equation (1)) and used for energetic or chemical purposes. This process typically employs fixed-bed reactors equipped with a bifunctional catalyst system [6,7]. The initial hydrolysis of DME to methanol requires an strongly acidic catalytic function (e.g., zeolites or γ-Al_2O_3), while the subsequent reforming step relies on metallic or oxidic active centres [10–12]. Copper and palladium systems have shown high conversion rates and hydrogen yields in the second step, but catalyst deactivation, primarily due to sintering or coking of the active sites, remains a challenge [13,14]. To address this, we recently proposed In_2O_3/ZrO_2 as an alternative catalyst in DME steam reforming, building on previous experience from the application in methanol synthesis and steam reforming [15–18]. When combined with γ-Al_2O_3 as the acidic support, the catalyst system demonstrated high hydrogen yields of 88 % over 425 h of continuous stable operation at 350 °C [19]. As can be seen from the reverse equation (1), DME steam reforming produces hydrogen not only from the delivered DME, but also from water, that has not to be transported, but is locally available at the destination. This results in the mentioned high technical hydrogen capacity of DME (equation (2)).

However, DME is gaseous at room temperature, which poses handling and storage challenges. Higher methyl ethers, so called polyoxymethylene dimethyl ethers (OMEs) exhibit boiling points above ambient temperature, while sustaining similar physico-chemical properties as DME. Dimethoxymethane (DMM, also known as the shortest polyoxymethylene dimethyl ether: OME_1) can be viewed as an extension of DME by an additional methoxy group. It is non-toxic, nor harmful for humans, nature or corrosive, and exhibits a technical hydrogen capacity of 21.0 %. With a boiling point of 42 °C, OME_1 is liquid at room temperature, while higher OMEs exhibit progressively higher boiling points.

In the case of OMEs, hydrogen can also be released by steam reforming. The steam reforming of OME_1 (OME_1-SR) has received little attention to date. Upon hydrolysis with water, OME_1 forms methanol and formaldehyde (equation (1)), each of which can later undergo steam reforming as described in equations (2) and (3). Thus far, investigations have primarily focused on copper-based catalysts with limited attention given to their long-term stability (Table S1) [20–22].

$$CH_3OCH_2OCH_3 + H_2O \rightleftharpoons 2\,CH_3OH + CH_2O \quad (1)$$

$$CH_3OH + H_2O \rightleftharpoons CO_2 + 3\,H_2 \quad (2)$$

$$CH_2O + H_2O \rightleftharpoons CO_2 + 2\,H_2 \quad (3)$$

The resulting overall reaction for OME_1 is given in equation (4). The reaction scheme transferred to higher OMEs results in the general OME_n steam reforming equation (5).

$$CH_3OCH_2OCH_3 + 4\,H_2O \rightleftharpoons 3\,CO_2 + 8\,H_2 \quad (4)$$

$$C_{n+2}H_{2n+6}O_{n+1} + (n+3)\,H_2O \rightleftharpoons (n+2)\,CO_2 + (2n+6)\,H_2 \quad (5)$$

However, to the best of our knowledge, the steam reforming of higher OMEs ($n \geq 2$) has not yet been reported in literature.

Potential side reactions of OME-SR include methanol decomposition (6), the formation of DME (7) and methyl formate (MF) (8), the reverse water-gas-shift reaction (9), MF decomposition (10) and methanation reaction (11).

$$CH_3OH \rightleftharpoons 2\,H_2 + CO \quad (6)$$

$$2\,CH_3OH \rightleftharpoons CH_3OCH_3 + H_2O \quad (7)$$

$$CH_2O + CH_2O \rightleftharpoons CH_3OCHO \quad (8)$$

$$CO_2 + H_2 \rightleftharpoons CO + H_2O \quad (9)$$

$$CH_3OCHO \rightleftharpoons CO + CH_3OH \quad (10)$$

$$CO_x + (2+x)H_2 \rightleftharpoons CH_4 + x\,H_2O \quad (11)$$

This study investigates the potential of OME_1 as a hydrogen carrier by analysing each step of the corresponding hydrogen transport cycle and performing a material and energy balance to determine its overall energy efficiency in comparison with methanol and dimethyl ether. Given that steam reforming of OMEs is crucial for hydrogen release but has so far been scarcely explored, this work presents an experimental investigation of this process. The objective was to identify a stable and technically applicable catalyst system that enables the efficient and selective conversion of OMEs into hydrogen and CO_2.First, the hydrolysis reaction was investigated using different acidic catalysts, followed by the evaluation of a binary In_2O_3/ZrO_2 catalyst for steam reforming. Particular attention was given to the long-term stability of this catalyst under technically relevant conditions. Finally, the steam reforming of higher OMEs, namely OME_2 and OME_3, was investigated to the best of our knowledge for the first time.

2. Methods

2.1. Materials

Different commercial catalyst pellets were used as supports and hydrolysis catalysts. γ-Aluminium oxide and zirconium oxide pellets (3 mm diameter) were obtained from Thermo Fisher Scientific, while titanium oxide pellets (3 mm diameter) were sourced from Alfa Aesar. The zeolite pellets (1.5 mm diameter) were obtained from Clariant. Indium oxide catalysts were synthesized using the precursor indium(III) nitrate hydrate (Puratronic™, 99.999 % metal basis, Thermo Fisher Scientific). Dimethoxymethane (DMM, OME_1) was purchased from Sigma-Aldrich (ReagentPlus®) and higher polyoxymethylene dimethyl ether (OME_2 and OME_3) were obtained from ASG Analytik-Service. High purity nitrogen (99.999 %, Air Liquide) was used as both carrier and calibration gas.

2.2. Catalyst synthesis and characterization

The In_2O_3/ZrO_2 catalyst used in this work was synthesized via wet impregnation. Indium(III) nitrate hydrate was dissolved in distilled

water at room temperature, followed by the addition of the zirconia support to the precursor solution. The solvent was subsequently removed using a rotary evaporator. The resulting material was dried in an oven for 12 h and then calcined. Calcination was carried out by heating with a rate of 2 K/min, up to a final temperature of 400 °C, which was held for 3 h. During this process, the furnace was continuously purged with synthetic air to maintain optimal calcination conditions.

The indium content of the synthesized catalyst samples was determined by ICP-OES using a PerkinElmer Plasma 400 spectrometer. For surface area analysis, the samples were first degassed at 250 °C for 12 h, followed by nitrogen adsorption measurements at −196 °C using a Quantachrome Quadrasorb SI-MP-8. The specific surface area was calculated according to the Brunauer–Emmett–Teller (BET) method. Powder X-ray diffraction was employed to investigate the crystal structure of the catalysts, using a Philips X'Pert Pro diffractometer with Cu-Kα radiation. Diffraction patterns were recorded with an angular step size of 0.017°, a counting time of 100 s per step, and a 2θ scan range from 10° to 90°.

2.3. Experimental evaluation

The steam reforming experiments were carried out in a stainless-steel fixed bed reactor (Halmosi, 30 mm inner diameter) equipped with a catalyst basket (volume: 20 cm^3). The desired amount of catalyst was loaded into the basket, and the reactor was purged with inert gas prior to each experiment. Unless otherwise specified, standard reaction conditions were set to 2 bar(a), 350 °C and a steam-to-OME_1 molar ratio of 5, with nitrogen added as internal standard at a concentration of 15 mol-%.

Reactants were vaporized separately and premixed before being introduced into the reactor (Fig. S1). Upon leaving the reactor, the product stream was directed through a condenser operated at 5 °C to enable phase separation. Gas-phase analysis was performed using an Agilent 490 Micro GC, employing nitrogen as the internal standard. The condensed liquid phase was collected and analysed offline using an Agilent 8890 GC with external calibration. Further details on the experimental setup are provided in the ESI. OME conversion was calculated according to equation (12):

$$X_{OME} = \frac{\dot{n}_{OME,in} - \dot{n}_{OME,out}}{\dot{n}_{OME,in}} \times 100 \quad (12)$$

The hydrogen yield Y_{H2} is defined as the ratio of hydrogen actually produced to the theoretically possible amount, and was estimated according to equation (13).

$$Y_{H2} = \frac{\dot{n}_{H2,out}}{\dot{n}_{OME,in}} \times \frac{1}{\nu_{i,H2}} \times 100 \quad (13)$$

Whereas $\nu_{i,H2}$ represents the number of hydrogen molecules produced by steam reforming under stoichiometric conditions (e.g. 8 for OME_1). The carbon yields are calculated according to equation (14):

$$Y_{i,C} = \frac{\dot{n}_{i,out}}{\dot{n}_{OME,in}} \times \frac{3}{\nu_{i,C}} \times 100 \quad (14)$$

$\nu_{i,C}$ represents the number of carbon atoms in the respective product molecule, for example, one for CO_2 and two for DME. The measured carbon-containing products included CO, CO_2, CH_4, methanol (MeOH), dimethyl ether (DME), and methyl formate (MF). Formaldehyde (FA) and methoxy methanol (MM) were detected in the offline GC analysis. However, reliable quantification of these compounds was not possible with the analytical method employed. Since no other carbon-containing products were detected during OME steam reforming, the unaccounted carbon (typically 5 - 20 % depending on the OME conversion) was attributed to the combined formation of FA and MM. For Figs. 4 and 6, the standard deviations of the gas-phase components were calculated from all measurements acquired within a 1-h period around the corresponding liquid sampling point.

3. Results

3.1. The OME/CO_2 transport cycle

This study investigates the potential of OMEs as hydrogen transport vectors for a future energy system. A hydrogen transport cycle employing OME_1 as the carrier is illustrated in Fig. 1 and comprises the following steps: (1) hydrogen production and CO_2 provision, (2) OME_1 synthesis, (3) OME_1 shipping and (4) hydrogen release via OME_1 steam reforming and CO_2 transport, back to the origin. In the following, each step is evaluated conceptually, and a preliminary energetic assessment of the overall transport cycle is presented.

3.1.1. Hydrogen production and CO_2 provision

Renewable hydrogen can be generated through water electrolysis or derived from other renewable sources such as biomass or recycled wastes. Among these options, water electrolysis powered by renewable energy such as solar, hydro and wind is considered one of the most sustainable hydrogen production technologies from a life cycle assessment perspective [23,24]. Favorable conditions for such systems, including high solar radiation and large available land areas, can be found in regions such as Australia, Namibia and Chile [24–26]. However, water electrolysis requires substantial quantities of purified water. In coastal regions such as Australia, seawater desalination may be necessary to meet this demand, particularly if the synthesis plant is located near a port for logistical reasons [27]. In this scenario, brine disposal from desalination is both, an environmental and economic challenge [28].

A large portion of the CO_2 required for OME_1 synthesis can be supplied through back-shipping from the hydrogen utilization site, while the remaining amount must be sourced from direct air capture (DAC), or biogenic emissions. Especially DAC is currently associated with high costs, although optimistic projections suggest a drastic decrease by 2050 [29–33]. Back-shipping can therefore significantly reduce the overall CO_2 supply costs [8]. Regardless of the source, all processes involved in renewable OME_1 production, including electrolysis and CO_2 supply, must be powered by renewable electricity, preferably from wind or solar energy, to ensure overall carbon neutrality.

3.1.2. OME_1 synthesis

There are several renewable pathways for producing OME_1, most of which rely on methanol as an intermediate. Consequently, the methanol itself must be synthesized from renewable hydrogen and recycled carbon dioxide, in catalytic hydrogenation reaction as displayed in equation (15):

$$CO_2 + 3\,H_2 \rightleftharpoons CH_3OH + H_2O \quad (15)$$

Due to the lower reactivity of CO_2 compared to CO, methanol synthesis from CO_2 typically requires larger reactor volumes and results in increased water formation [34]. Furthermore, despite recent advances, CO_2 hydrogenation to methanol remains technically challenging due to kinetic limitations and catalyst requirements. However, this route offers several advantages: it exhibits higher selectivity, improved carbon utilization efficiency, and operates under milder reaction conditions, as the reaction is less exothermic than CO-based methanol synthesis. Currently, methanol synthesis from CO_2 is economically viable only under specific conditions, namely, if green hydrogen is available at low cost or if CO_2 emissions are taxed (at least 300 \$ ton^{-1}) [35].

The established commercial route for synthesizing OME_1 starts from methanol and follows a two-step process. In the first step, formaldehyde is produced from methanol, in the second step, formaldehyde is acetalized with methanol to yield OME_1. Both reactions can be conducted in a single reaction step without isolation of formaldehyde (equation (16)).

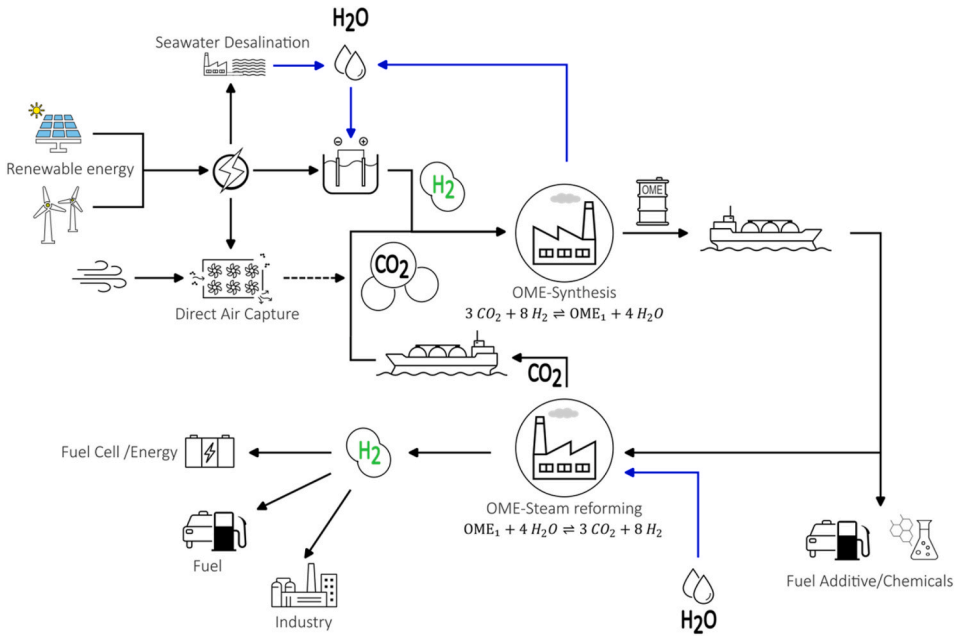


Fig. 1. Proposed OME/CO_2 cycle for the transport of renewable hydrogen.

$$3\ CH_3OH + 0.5\ O_2 \rightleftharpoons CH_3OCH_2OCH_3 + 2\ H_2O \quad (16)$$

This reaction has been demonstrated in continuous-flow setups at atmospheric pressure and temperatures ranging from 120 to 280 °C, employing Ru-, Re-, Mo- or V-based catalysts [36–40]. The oxygen required for methanol oxidation (equation (17)) is generated as a by-product during water electrolysis, eliminating the need for an external oxygen supply. While methanol oxidation offers high yields, it causes a significant explosion risk due to the involvement of oxygen in the gas phase. Additionally, the reaction generates large amounts of water as a by-product.

In the context of the proposed energy transport scenario, the generated water can be reused for electrolysis to produce hydrogen on site, reducing the demand for desalinated water by approximately 56 % and thereby lowering the associated environmental impact. In the two-step synthesis process, nine hydrogen molecules are required to produce one OME_1 molecule, which subsequently releases eight hydrogen molecules at the destination site. The remaining hydrogen is bound in the water formed during synthesis, which is recycled to the electrolysis step but contributes to an increased overall energy demand.

Several novel one-step pathways to synthesize OME_1 (which would not require such an additional hydrogen molecule) have been proposed, recently, to improve process efficiency and integration [41–44]. One such "direct route" is the dehydrogenative coupling, proceeding via CO_2 hydrogenation in the presence of methanol over Cu/SiO_2 catalysts [45]. This process can achieve high selectivity at around 240 °C and 2 MPa, but it is limited by chemical equilibrium and has so far only been demonstrated in lab-scale batch reactors. A similar approach involves the catalytic hydrogenation of CO_2 with H_2 to generate formaldehyde, which is then immediately trapped *in-situ* on an acidic catalyst, reacting with methanol to form OME_1. These systems typically rely on homogeneous catalysts, such as Ru(triphos)(tmm) in combination with Al$(OTf)_3$, and operate under conditions of 80 °C, 20 bar CO_2 and 60 bar H_2 [46]. Although significant progress has been made in these reductive processes in recent years, they have not yet been developed to a technical-industrial level. For this feasibility study, the established two-step method reported by Schemme et al. was adopted [47].

3.1.3. Shipping of the hydrogen carrier OME_1

After the production, OME_1 and water are separated easily due to a large difference in boiling points (100 °C vs. 42 °C @ 1 atm). In the proposed scenario, OME_1 with a technical hydrogen capacity of 21.0 % is transported over long distances by ship. Compared to DME and methanol, OME_1 exhibits the highest liquid density at 20 °C, with 0.86 kg l^{-1} (0.73 kg l^{-1} for liquefied DME and 0.79 kg l^{-1} for methanol). Being liquid at room temperature, OME_1 can be pumped and shipped using the same vessel employed for CO_2 back-shipping. Such liquefied CO_2 (LCO_2) carriers are, for example, currently being developed and launched by Mitsubishi [48]. The boil-off rate of liquid compounds typically depends on their vapor pressure. Although no data are available for OME_1, it can be estimated to be of the same order of magnitude as that of methanol, which has a boil-off rate of approximately 0.0005 % d^{-1} [5,49]. At the destination, OME_1 can be used as a sustainable combustion fuel or additive, as a chemical solvent or substrate or the hydrogen can be recovered through steam reforming [50–52].

3.1.4. Steam reforming of OME_1 to release hydrogen

For the steam reforming process, water must be supplied in addition to OME_1 in order to release hydrogen. Since water is locally available at the reforming site, only a fraction of the produced hydrogen originates from the shipped OME_1 itself, while the remainder is derived from the added water. The recovered hydrogen can then be used for energy generation via fuel cells, as a feedstock for the synthesis of more complex chemicals, or directly as a fuel [53–56]. During this process, CO_2 is produced, captured, and stored for transport back to the synthesis site, completing a carbon cycle that, in principle, can achieve net-zero emissions. However, as shown Table S1, the steam reforming of OME_1 has been scarcely studied, and experimental validation, particularly regarding long-term stability, is needed. This is addressed in a later section of the paper.

To assess the feasibility of the OME_1/CO_2 transport cycle, a comparative analysis of the material and energy balances of OME_1 was conducted and compared against DME and methanol as hydrogen carriers. The calculations are based on the methodology described by Schühle et al., assuming the release of one ton of hydrogen at the point of utilization with CO_2 back-shipping [8]. All relevant assumptions are listed in Tables S3 and S4 in the supplementary information. The results are presented in Table 1.

Regarding the properties of the three carriers, OME_1 has the lowest hydrogen content by weight but, due to the additional conversion of

Table 1
Properties, material- and energy balance for methanol, dimethyl ether and dimethoxymethane (established two-step route with methanol oxidation and direct synthesis from H_2 and CO_2) as a hydrogen carrier molecule.

	Unit	MeOH	DME[a]	OME_1 (established)	OME_1 (direct)
Carrier properties					
$w_{H2,\ carrier}$[b]	% (t_{H2} $t_{carrier}^{-1}$)	12.50	13.04	10.51	10.51
$w_{H2,\ technical}$	% ($t_{H2,\ released}$ $t_{carrier}^{-1}$)	18.75	26.09	21.02	21.02
Liquid density	kg m^{-3}	805	735[c]	860	860
Volumetric storage density	g_{H2} $l_{carrier}^{-1}$	150.94	191.76	180.77	180.77
Lower heating value	MJ kg^{-1}	19.9	28.9	23.3	23.3
Material balance					
H_2 released	t	1	1	1	1
Carrier demand	t_X $t_{H2,\ released}^{-1}$	5.49	3.95	4.90	4.90
H_2O demand for production (with recycle)	t_{H2O} $t_{H2,\ released}^{-1}$	7.21	5.66	5.75	5.66
CO_2 demand (with back-shipping)	t_{CO2} $t_{H2,\ released}^{-1}$	0.23	0.23	0.25	0.25
O_2 side product	t_{O2} $t_{H2,\ released}^{-1}$	4.12	4.12	3.61	4.12
Energy balance					
Water desalination	MWh_{el} $t_{H2,\ released}^{-1}$	0.36	0.28	0.29	0.28
Electrolyzer	MWh_{el} $t_{H2,\ released}^{-1}$	51.50	51.50	57.75	51.50
Direct air capture	MWh_{el} $t_{H2,\ released}^{-1}$	0.11	0.11	0.13	0.13
	MWh_{th} $t_{H2,\ released}^{-1}$	0.34	0.34	0.38	0.38
Synthesis	MWh_{el} $t_{H2,\ released}^{-1}$	0.851	0.854	1.11	1.11
	MWh_{th} $t_{H2,\ released}^{-1}$	−2.67	−1.14	−1.35	−1.35
Shipping	MWh $t_{H2,\ released}^{-1}$	1.44	1.13	1.20	1.20
Steam reforming	MWh_{th} $t_{H2,\ released}^{-1}$	6.27	6.36	6.08	6.08
Liquification of CO_2	MWh $t_{H2,\ released}^{-1}$	1.68	1.68	1.89	1.89
Total energy demand					
Carrier production	MWh $t_{H2,\ released}^{-1}$	50.49	51.95	58.31	52.05
Transport and H_2 release	MWh $t_{H2,\ released}^{-1}$	9.38	9.18	9.17	9.17
Energy efficiency[d]	%	55.09	53.96	48.88	53.87

[a] According to Schühle et al. [8].
[b] $w_{H2,carrier} = \frac{m_{H2,Carrier}}{m_{Carrier}}$.
[c] Liquefied.
[d] $\eta_{Energy} = \frac{\sum m_{H2} \cdot LHV_{H2}}{\sum Q_j + \sum W_k + \sum m_l \cdot LHV_l}$

water in the steam reforming process, releases about 11 % more hydrogen per ton of carrier at the point of use, compared to methanol. In terms of liquid density, OME_1 has the highest value, while its lower heating value and carrier demand fall between those of methanol and DME. The first notable differences between the established and the direct OME_1 synthesis routes appear in the water demand. In the established route, more water is generated during synthesis but also more is consumed during electrolysis, resulting in a higher overall demand. In contrast, the direct synthesis route shows a water demand similar to that of DME. Methanol exhibits the highest water demand, as less recyclable water is formed during its synthesis. The CO_2 demand is slightly higher for OME_1, although the difference is marginal since most CO_2 is back-shipped in our scenario, why only small losses need to be compensated. Differences in O_2 side production occur only for the established OME_1 route due to oxygen consumption in methanol oxidation. However, most of the oxygen produced in an electrolyzer is anyhow vented and therefore oxygen can often not be considered as a valuable product.

Based on these material requirements, the electric and thermal energy balances for each process step were calculated. Energy consumption for water desalination and DAC is minor compared to other process steps, such as electrolysis, where all routes except the established two-step OME_1 synthesis require a similar amount of energy. The established route demands more hydrogen for synthesis than is released during reforming, leading to higher specific energy requirements for electrolysis per amount of released hydrogen. Although methanol has the lowest reaction enthalpy (approximately 131 kJ mol^{-1}), the highest overall heat release during synthesis is observed for methanol formation. In contrast, DME and OME_1 provide less useable heat during their synthesis, even though their reaction enthalpies are higher (approximately 273 kJ mol^{-1} and 340 kJ mol^{-1}, respectively). This is because the formation of DME and OME_1 involves additional process steps, including intermediate formation, separation, and product purification, which consume a significant fraction of the theoretically available reaction heat. The shipping energy demand is largest for methanol, as its lower technical hydrogen capacity necessitates transporting a larger mass. Steam reforming of all carriers was simulated using Aspen Plus, showing that OME_1 performs between DME and methanol in terms of energy requirements. The energy required for CO_2 liquefaction is slightly higher for OME_1, as a larger amount of CO_2 must be back-shipped. Overall, the total energy demand for carrier production is lowest for methanol and highest for the established OME_1 process, primarily due to the greater energy consumption of the electrolyzer. In contrast, for transport and hydrogen release, the trend is reversed: methanol shows the highest energy demand, while OME_1 requires the least. The total energy efficiency of the established OME_1 route is around 49 %, which is lower than that of methanol and DME. However, when OME_1 is synthesized directly from CO_2 and H_2 without intermediate O_2 formation, the overall energy efficiency becomes comparable to methanol and DME, highlighting the importance of improving this process step. To assess the robustness of the proposed transport cycle, a sensitivity analysis was conducted, which is provided in the ESI.

Another major challenge for OME_1 lies in the limited research on its steam reforming reaction, which would be crucial for hydrogen release in the presented cycle. While several studies have addressed its synthesis, only few have explored the reforming process in detail, especially concerning catalyst long-term stability. Therefore, in this work, we investigate OME_1 steam reforming using a new catalyst system, focusing on reaction conditions, long-term stability, and the potential influence of synthesis-derived impurities such as higher OMEs.

3.2. Experimental studies of OME steam reforming

3.2.1. Hydrolysis of dimethoxymethane

We initially focused on studying reaction (1), the hydrolysis of OME_1 to methanol and formaldehyde. Previous experience with DME steam

reforming (DME-SR) has shown that acidic aluminium oxide is a highly effective catalyst for this reaction step, which is why we selected it as our benchmark [19]. Fig. 2 a) demonstrates an increase in OME_1 conversion from 25 % to 90 % with rising temperature from 200 to 400 °C. By increasing the catalyst amount up to 3 g, complete conversion is achieved at 350 °C. Notably, no hydrogen formation is observed in the hydrolysis studies with Al_2O_3. The corresponding carbon yields are depicted in Fig. 2 b). No significant CO_2 is formed, as no hydrogen is produced, and methane formation is also negligible. The yield of methyl formate, generated from formaldehyde (reaction (8)), increases up to 250 °C and then declines at higher temperatures [57].

Simultaneously, carbon monoxide becomes more present, presumably due to the decomposition of formaldehyde (reaction (10)). Methanol yield rises up to 300 °C before decreasing again, primarily due to the onset of DME formation at 350 °C, driven by reaction (7).

An increase in carbon deposits on the Al_2O_3 catalyst was visually observed at elevated temperatures (Fig. S2). To determine whether the coking is caused by the specific catalyst, we tested alternative materials for the OME_1 hydrolysis, specifically zirconia (ZrO_2), titania (TiO_2) and a ZSM-5 zeolite. Fig. 3 shows the OME_1 conversion as well as the corresponding H_2 and carbon product yields at 350 °C using 3 g of catalyst. Methane and methyl formate yields remained below 1 % for all materials and are therefore not included. Interestingly, a conversion of 46 % was achieved even in the absence of a catalyst, indicating that the reaction proceeded solely due to thermal effects. Among the tested catalysts, Al_2O_3, zeolite, and TiO_2 showed nearly complete OME_1 conversion but also formation of DME as a by-product. It should be noted that DME

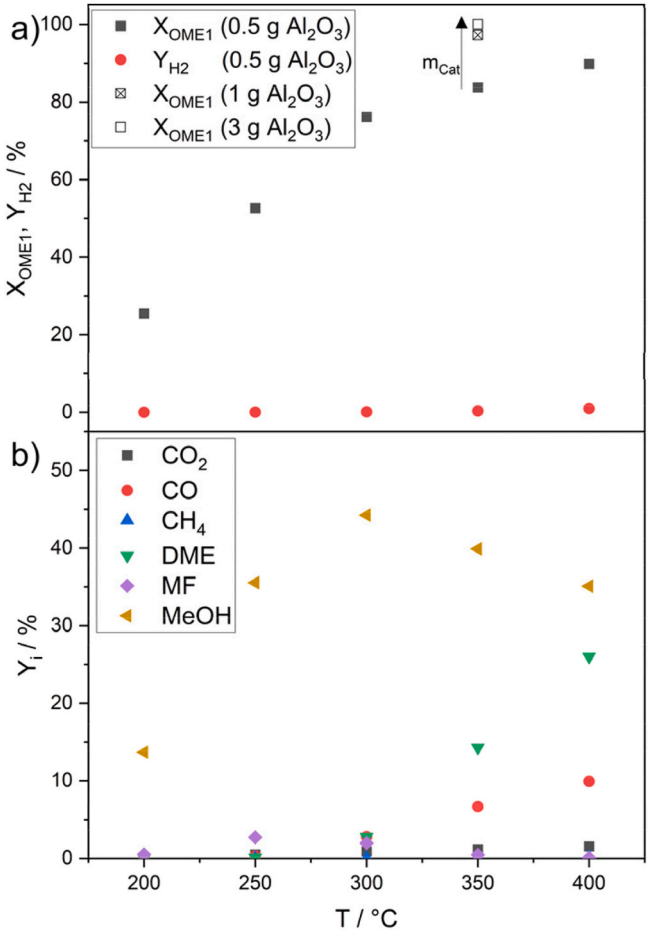


Fig. 2. Effects of process temperature on a) OME_1 conversion and H_2 yield; b) carbon yield (p = 2 bar(a); n_{H2O}:n_{OME1} = 5:1; m_{Al2O3} = 0.5 g; Missing C: FA + MM).

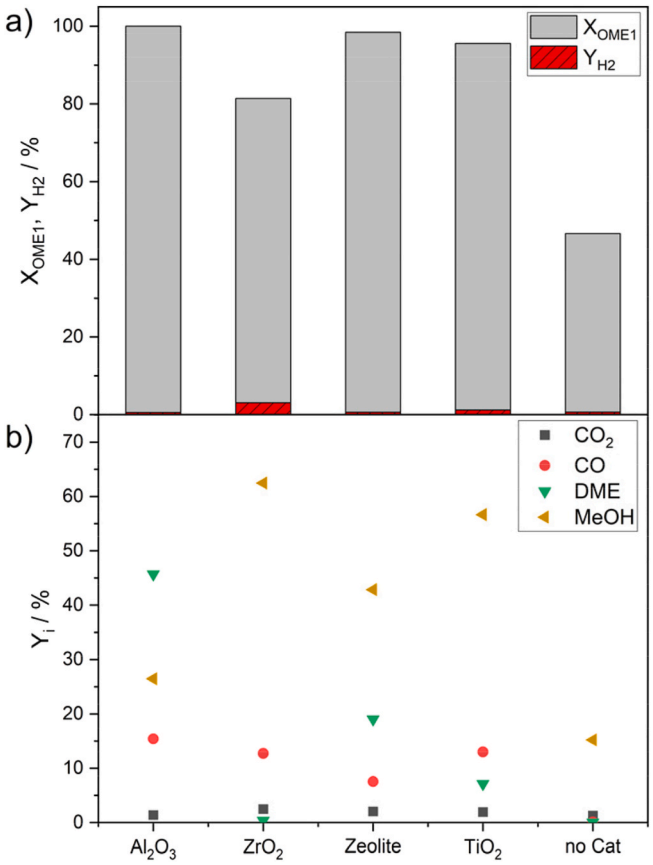


Fig. 3. Effects of different hydrolysis catalysts on a) OME_1 conversion and H_2 yield; b) carbon yield (p = 2 bar(a); n_{H2O}:n_{OME1} = 5:1; T = 350 °C; WHSV = 8.6 g_{Ed} g_{Cat}^{-1} h^{-1}; m_{Cat} = 3 g; CH_4 and MF yield below 1 %; Missing C: FA + MM).

formation is undesirable, as it consumes methanol that is intended for conversion to hydrogen and CO_2 in the subsequent steam reforming step. In contrast, ZrO_2, being less acidic, showed slightly lower OME_1 conversion but did not catalyse DME formation [58]. Additionally, only the zirconia-based catalyst retained its white colour after 5 h on stream, indicating significantly lower carbon deposition compared to the other materials.

Using a higher amount of zirconia catalyst (9 g) resulted in nearly complete conversion. Interestingly, zirconia also seems to promote methanol decomposition to a slight degree, as indicated by the small quantities of hydrogen detected (Fig. S3). The much higher CO formation is likely due to the decomposition of methyl formate (reaction (10)), which proceeds almost completely at 350 °C. Although ZrO_2 exhibits lower activity in OME_1 hydrolysis than more acidic materials, it was identified as the most suitable catalyst for OME_1 hydrolysis due to its reduced side-product formation and lower coking tendency.

3.2.2. *Steam reforming of dimethoxymethane*

Based on our previous studies with DME, an In_2O_3/ZrO_2 catalyst was investigated for OME_1 steam reforming in the present work [19]. Since ZrO_2 itself had previously proven to be a suitable material for OME_1 hydrolysis, the aim was to examine whether high OME_1 conversions and hydrogen yields could be achieved using In_2O_3/ZrO_2 without the addition of an acidic component. Simulations performed using Aspen Plus, together with the literature data summarized in Table S1, indicate that complete conversion of OME_1 to hydrogen is thermodynamically feasible.

Fig. 4 shows the results with 1 g of In_2O_3/ZrO_2 with an indium loading of 1.81 wt% in a temperature range of 200 to 400 °C. OME_1 conversion steadily increases with rising temperature, while substantial

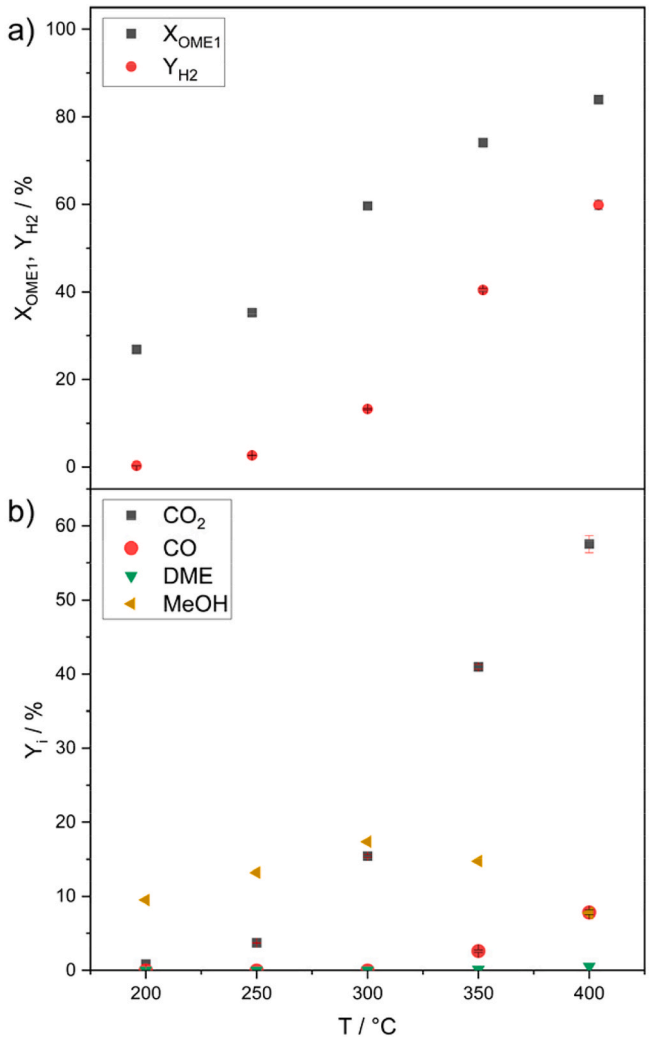


Fig. 4. Effects of process temperature on a) OME_1 conversion and H_2 yield; b) carbon yield (p = 2 bar(a); n_{H2O}:n_{OME1} = 5:1; WHSV = 8.6 g_{Ed} g_{Cat}^{-1} h^{-1}; $m_{In2O3/ZrO2}$ = 3 g (1.81 wt% Indium); CH_4 and MF yield below 1 %; Missing C: FA + MM).

H_2 and CO_2 formation begins at 300 °C. At 350 °C, CO is detected, likely formed via the endothermic reverse water-gas shift (rWGS) reaction. Concurrently, methanol yield begins to decline from 300 °C onwards. Undesired by-products such as DME, CH_4, and methyl formate are detected only in negligible amounts. OME_1 steam reforming proceeds with high selectivity and hydrogen yield over the In_2O_3/ZrO_2 catalyst alone. In contrast to DME, no additional acidic catalyst is necessary, indicating that OME_1 hydrolysis is kinetically facilitated.

To improve hydrogen yield, we systematically varied the indium content in the catalysts. As shown in Fig. S4, no hydrogen is produced in the absence of indium, confirming its essential function in the methanol steam reforming (MSR). Upon adding indium, hydrogen generation starts and doesn't improve significantly with higher loadings. This aligns with previous reports for methanol synthesis and DME steam reforming [19,59,60].

Another approach to influence hydrogen yield is to vary the steam-to-OME_1 ratio, since water acts as a reactant in both the hydrolysis and steam reforming steps. As shown in Fig. S5, no significant changes in hydrogen yield or OME_1 conversion were observed upon increasing the ratio from four (stochiometric) to eight. While the CO_2 and methanol yields remained relatively constant at around 60 % and 20 %, respectively, the CO yield steadily decreased from 1.1 % to 0.5 % with a higher steam-to-OME1 ratio. This trend can be attributed to the rWGS reaction (9), which is increasingly suppressed in the presence of excess water, thereby favouring the formation of H_2 and CO_2. This effect is likely to become even more pronounced at higher conversions, as the reaction mixture becomes progressively depleted in water.

3.2.3. *Long-term catalyst stability in OME steam reforming*

Since this study aims to investigate OME_1 steam reforming under technically relevant hydrogen yields and to assess long-term stability, the catalyst amount was increased to 20 g and the time on stream time was extended to 380 h. The results are presented in Fig. 5. The conversion and yields are stable, with some fluctuations particularly noticeable between 125 and 225 h on stream. These fluctuations can be attributed to slight pulsations of the evaporator upstream of the reactor. Overall, both conversion and product yield remained stable, suggesting the absence of catalyst deactivation. A shutdown was performed between 35 and 45 h to examine the dynamic behavior of the system. Upon restarting the reaction under identical conditions, no loss in catalyst performance was observed, confirming its high stability and robustness under fluctuating operating conditions.

Throughout the experiment, the CO_2 yield lies at ~73 %, while CO remains at ~10 %. This CO fraction could be further reduced by implementing a downstream water-gas shift reactor operating at lower temperatures [19]. Methanol content in the product stream is low, with a yield < 3 %. Other carbon-containing byproducts such as dimethyl

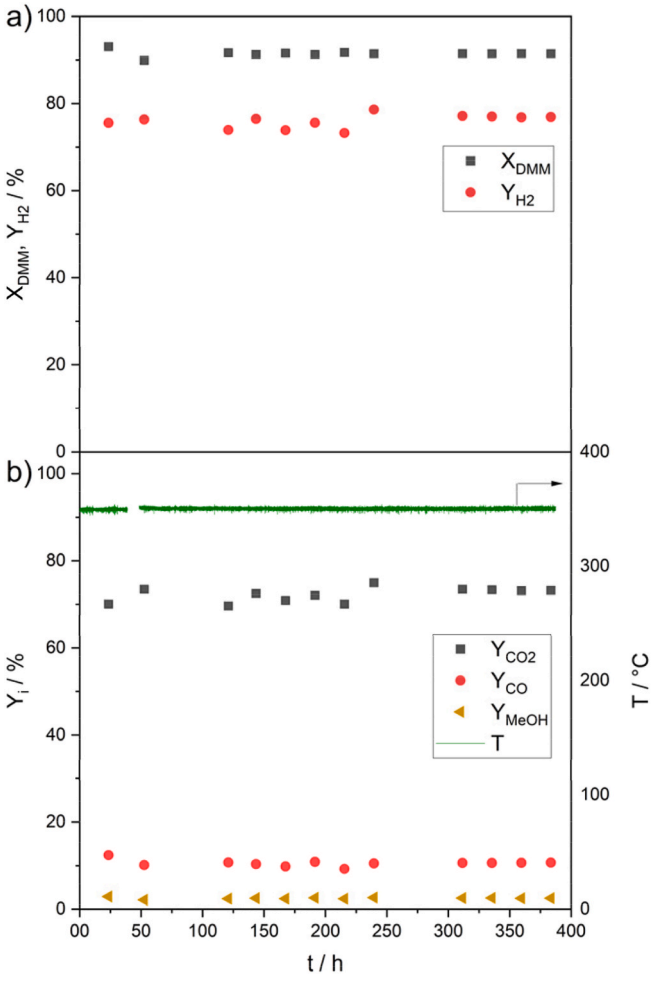


Fig. 5. Investigation of long-term stability of the In_2O_3/ZrO_2 catalyst. a) OME_1 conversion and H_2 yield; b) carbon yield and reaction temperature (p = 2 bar (a); n_{H2O}:n_{OME1} = 5:1; T = 350 °C; WHSV = 1.29 g_{Ed} g_{Cat}^{-1} h^{-1}; $m_{In2O3/ZrO2}$ = 20 g (2.66 wt% Indium); DME, CH_4 and MF yield below 1 %; Missing C: FA + MM).

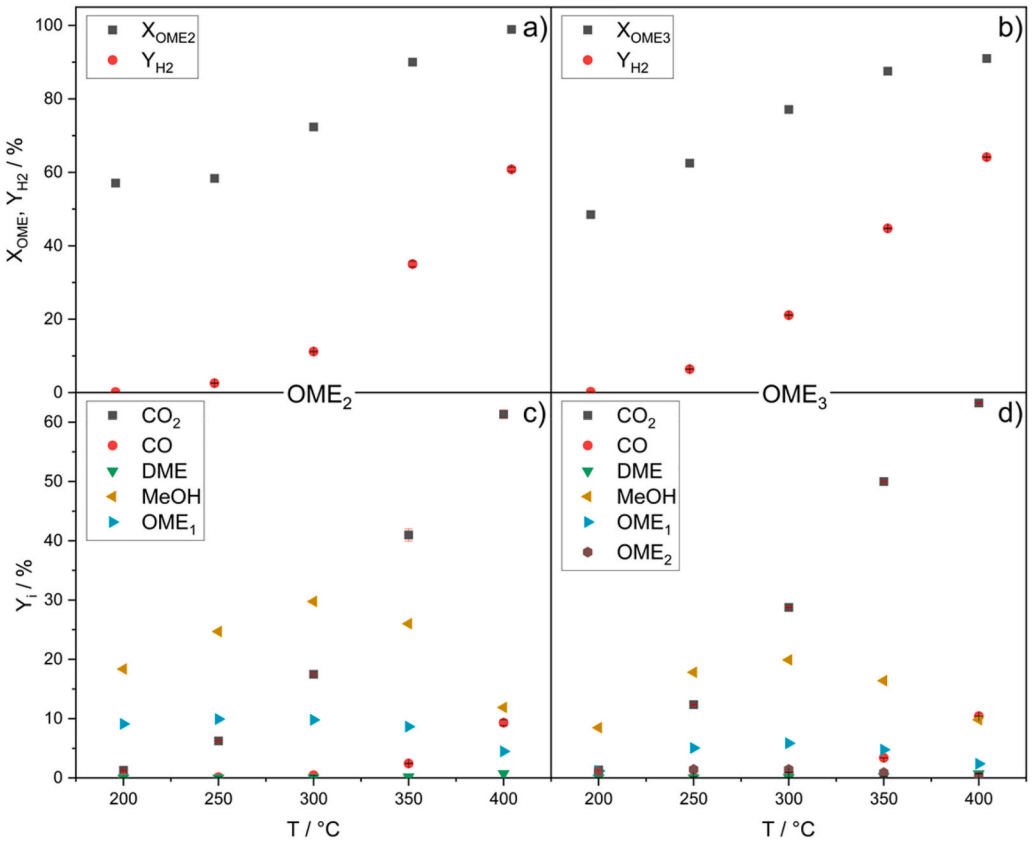


Fig. 6. OME conversion, H_2 and carbon yields for a) & c) OME_2 (n_{H2O}:n_{OME2} = 6:1; $m_{In2O3/ZrO2}$ = 2.8 g (2.57 wt% Indium) and b) & d) OME_3 (n_{H2O}:n_{OME3} = 7:1; $m_{In2O3/ZrO2}$ = 2.7 g (2.57 wt% Indium) for 200 to 400 °C (p = 2 bar(a); WHSV = 8,6 g_{Ed} g_{Cat}^{-1} h^{-1}); CH_4 and MF yield below 1 %; Missing C: FA + MM.

ether, methane, and methyl formate are detected at yields below 0.5 %, confirming CO as the dominant carbonaceous byproduct. A hydrogen productivity of 3.1 g_{H2} g_{In}^{-1} h^{-1} (34 $l_{N,H2}$ g_{In}^{-1} h^{-1}) was sustained over more than 380 h using the indium catalyst, which is comparable to values reported for DME steam reforming and represents the highest productivity achieved to date for OME_1 steam reforming (Table S1). As expected, reducing the WHSV from 8.6 to 1.3 g_{Ed} g_{Cat}^{-1} h^{-1} relatively increased the hydrogen yield by 87 %, from 40.5 % (Fig. 4) to 75.9 %, due to the longer residence time of the reactants. Even higher hydrogen output could potentially be achieved by increasing the reaction temperature or the steam-to-OME_1 ratio to suppress CO formation, though this would increase the energy required for heating and vaporization. Post-reaction N_2-physisorption and ICP-OES analyses of the spent In_2O_3/ZrO_2 catalyst after 380 h on stream revealed no significant changes in specific surface area or indium content (Fig. S6), further confirming the excellent catalyst stability under the investigated reaction conditions.

3.2.4. *Steam reforming of OME_2 and OME_3*

During the synthesis of OME_1 from methanol and formaldehyde, higher OMEs are formed as by-products following a Schulz-Flory distribution and remain in the product mixture [61]. This makes it relevant to study their behavior under steam reforming conditions, if this mixture is used as a hydrogen carrier. Fig. 6 presents the steam reforming performance of OME_2 and OME_3 in the temperature range of 200 - 400 °C. The catalyst loading was adjusted to ensure comparable weight hourly space velocities (WHSV) to Fig. 4. Fig. 6 a) and b) show the respective conversion and hydrogen yield. Both OME_2 and OME_3 exhibit a behaviour similar to OME_1, achieving conversions > 80 % at temperatures above 350 °C, with hydrogen yields of up to 60 %. The corresponding carbon yields are depicted in Fig. 6 c) and d). The observed side products are comparable to those formed during OME_1 steam reforming, with the addition of shorter OME species appearing as intermediates when OME_2 or OME_3 undergo steam reforming. In OME_2 steam reforming, approximately 10 % of OME_1 is formed, remaining nearly constant across the temperature range of 200 - 350 °C. In the case of OME_3 steam reforming, OME_1 formation is lower, reaching up to 5 %, accompanied by OME_2 formation with a maximum of 1.4 % at 300 °C.

With both reactants, methanol is the main intermediate product in the reactor outlet, showing a maximum around 300 °C. For OME_3, the methanol concentration is generally lower, as the molecule contains more -CH_2O- groups that decompose to formaldehyde and fewer terminal methoxy groups generating methanol as intermediate. The CO_2 formation follows the same trend as the hydrogen yield, by increasing exponentially with temperature. Although OME_3 exhibits higher H_2 and CO_2 yields than OME_2 between 250 and 350 °C, no clear correlation between OME chain length and reforming performance can be derived from the present results, as OME_1 showed comparable or even higher yields under the investigated conditions. While the higher formaldehyde fraction in longer-chain OMEs may influence their reforming behavior, the observed differences are small and do not allow definitive mechanistic conclusions. At higher temperatures CO formation increases, while all other by-products gradually decrease. The small standard deviations shown in Figs. 4 and 6 demonstrate the high stability of the gas-phase composition throughout all OME steam reforming experiments. Overall, both compounds show comparable or even facilitated reforming behaviour compared to OME_1, suggesting that a synthesis mixture does not necessarily require separation before being processed in the same reactor.

4. Conclusions

In this contribution, OMEs were proposed as chemical vector for long distance hydrogen shipping. For OME_1, the shortest representative of

these compounds, this work introduces all steps of a proposed transport cycle and evaluates them energetically. At favorable locations for renewable energy production, OME_1 can be synthesized from green hydrogen and CO_2 and subsequently transported using existing infrastructure to regions with high energy demand. There, it can either be converted via steam-reforming back to hydrogen and CO_2 or directly utilized as a fuel or chemical feedstock. After hydrogen release, the resulting CO_2 can be separated, liquefied, and returned to the production site in the same ship, thereby closing the carbon loop.

A comparison of the material and energy balances with methanol and DME shows that OME_1 offers an attractive technical hydrogen capacity and can be handled using conventional transport infrastructure but exhibits a lower overall energy efficiency. By switching from the established two-step synthesis to a direct synthesis route from CO_2 and H_2, the overall energy efficiency becomes comparable to that of DME and methanol, mainly as less hydrogen is converted into water in direct synthesis. However, direct synthesis is not yet available at large scale and remains at an early stage of development, although significant progress has been achieved at the laboratory scale. In contrast, the steam reforming reaction responsible for hydrogen release has received little attention for OME_1 and, to the best of our knowledge, has never been investigated for higher OMEs.

Therefore, we demonstrated and investigated these reactions using an In_2O_3/ZrO_2 catalyst. We paid special attention to conduct our steam reforming experiments at technically relevant conditions and to evaluate long-term stability of the catalyst. Unlike for DME, the hydrolysis of OMEs was shown to proceed efficiently without the need for an additional acidic catalyst. Although acidic catalysts can enhance the hydrolysis activity, their use may promote the formation of undesired side products, such as CO and DME. The In_2O_3/ZrO_2 catalyst, in contrast, is sufficient to catalyse both the hydrolysis of OME and the subsequent steam reforming of the resulting intermediates, methanol and formaldehyde. A variation in indium loading had little effect on conversion or hydrogen yield, while increasing the steam-to-OME_1 ratio can suppress undesired CO formation. The In_2O_3/ZrO_2 catalyst demonstrated stable operation over 380 h of time-on-stream, achieving a hydrogen yield of 78 % and a productivity of 34 $l_{N,H2}\ g_{In}^{-1}\ h^{-1}$. The steam reforming of OME_2 and OME_3 proceeds with similar activity compared to OME_1; however, it appears that the increased chain length leads to higher hydrogen yields under the same conditions.

CRediT authorship contribution statement

Fabian Kroll: Writing – original draft, Visualization, Validation, Methodology, Investigation. **Michael Geißelbrecht:** Writing – review & editing, Supervision, Project administration. **Patrick Schühle:** Writing – review & editing, Supervision, Resources, Project administration, Funding acquisition, Conceptualization.

Data availability

Data is available on the data repository Zenodo (https://doi.org/10.5281/zenodo.15798900).

Declaration of generative AI and AI-assisted technologies in the manuscript preparation process

During the preparation of this work the authors used ChatGPT and DeepL to assist with language editing, text refinement and improving clarity and readability. After using this tool/service, the authors reviewed and edited the content as needed and take full responsibility for the content of the published article.

Declaration of competing interest

The authors declare that they have no known competing financial interests or personal relationships that could have appeared to influence the work reported in this paper.

Acknowledgements

The authors gratefully acknowledge the funding of the Bavarian Ministry of Economic Affairs, Regional Development and Energy (Grant number: 84-6665a2/164/4). The authors further gratefully acknowledge the Federal Ministry of Research, Technology, and Space for funding of the BMFTR Junior Research Group FAIR-H2 (Grant number: 03SF0730).

Appendix A. Supplementary data

Supplementary data to this article can be found online at https://doi.org/10.1016/j.ijhydene.2026.157502.

References

[1] European Commission. The European green deal. Available from: https://commission.europa.eu/strategy-and-policy/priorities-2019-2024/european-green-deal_en; May 13, 2025.
[2] International Energy Agency. Global hydrogen review. 2024 [May 13, 2025]; Available from: https://www.iea.org/reports/global-hydrogen-review-2024.
[3] d'Amore-Domenech R, Meca VL, Pollet BG, Leo TJ. On the bulk transport of green hydrogen at sea: comparison between submarine pipeline and compressed and liquefied transport by ship. Energy 2023;267:126621.
[4] Okunlola A, Giwa T, Di Lullo G, Davis M, Gemechu E, Kumar A. Techno-economic assessment of low-carbon hydrogen export from Western Canada to Eastern Canada, the USA, the Asia-Pacific, and Europe. Int J Hydrogen Energy 2022;47(10):6453–77.
[5] Al-Breiki M, Bicer Y. Investigating the technical feasibility of various energy carriers for alternative and sustainable overseas energy transport scenarios. Energy Convers Manag 2020;209:112652.
[6] Catizzone E, Freda C, Braccio G, Frusteri F, Bonura G. Dimethyl ether as circular hydrogen carrier: catalytic aspects of hydrogenation/dehydrogenation steps. J Energy Chem 2021;58:55–77.
[7] Pawelczyk E, Łukasik N, Wysocka I, Rogala A, Gębicki J. Recent progress on hydrogen storage and production using chemical hydrogen carriers. Energies 2022;15(14):4964.
[8] Schühle P, Stöber R, Semmel M, Schaadt A, Szolak R, Thill S, et al. Dimethyl ether/CO 2 – a hitherto underestimated H 2 storage cycle. Energy Environ Sci 2023;16(7):3002–13.
[9] Azizi Z, Rezaeimanesh M, Tohidian T, Rahimpour MR. Dimethyl ether: a review of technologies and production challenges. Chem Eng Process Process Intensif 2014;82:150–72.
[10] Ledesma C, Ozkan US, Llorca J. Hydrogen production by steam reforming of dimethyl ether over Pd-based catalytic monoliths. Appl Catal B Environ 2011;101(3–4):690–7.
[11] Wang S-S, Song Y-H, Zhao Y-H, Liu C, Xiao Y-S, Zhang Q, et al. Amorphous silica-alumina composite with regulated acidity for efficient production of hydrogen via steam reforming of dimethyl ether. Catal Today 2020;351:68–74.
[12] Yoshida H, Iwasa N, Akamatsu H, Arai M. Stable and selective hydrogen production through steam reforming of dimethyl ether with an Al 2 O 3 and PdZn composite catalyst. Int J Hydrogen Energy 2015;40(16):5624–7.
[13] Ledesma C, Llorca J. Dimethyl ether steam reforming over Cu–Zn–Pd/CeO 2 –ZrO 2 catalytic monoliths. The role of Cu species on catalyst stability. J Phys Chem C 2011;115(23):11624–32.
[14] Oar-Arteta L, Remiro A, Vicente J, Aguayo AT, Bilbao J, Gayubo AG. Stability of CuZnOAl2O3/HZSM-5 and CuFe2O4/HZSM-5 catalysts in dimethyl ether steam reforming operating in reaction–regeneration cycles. Fuel Process Technol 2014;126:145–54.
[15] Martin O, Martín AJ, Mondelli C, Mitchell S, Segawa TF, Hauert R, et al. Indium oxide as a superior catalyst for methanol synthesis by CO 2 hydrogenation. Angew Chem 2016;128(21):6369–73.
[16] Barbosa RL, Papaefthimiou V, Law YT, Teschner D, Hävecker M, Knop-Gericke A, et al. Methanol steam reforming over indium-promoted Pt/Al 2 O 3 catalyst: nature of the active surface. J Phys Chem C 2013;117(12):6143–50.
[17] Köwitsch N, Thoni L, Klemmed B, Benad A, Paciok P, Heggen M, et al. Proving a paradigm in methanol steam reforming: Catalytically highly selective in x Pd y/In 2 O 3 interfaces. ACS Catal 2021;11(1):304–12.
[18] Rameshan C, Lorenz H, Armbrüster M, Kasatkin I, Klötzer B, Götsch T, et al. Impregnated and Co-precipitated Pd-Ga2O3, Pd-In2O3 and Pd-Ga2O3-In2O3 catalysts: influence of the microstructure on the CO2 selectivity in methanol steam reforming. Catal Lett 2018;148(10):3062–71.
[19] Stöber R, Seidl F, Hoffmann E, Wasserscheid P, Schühle P. A highly durable catalyst system for hydrogen production from dimethyl ether. Sustain Energy Fuels 2024;8(8):1740–9.

[20] Badmaev SD, Pechenkin AA, Belyaev VD, Sobyanin VA. Hydrogen production by steam reforming of dimethoxymethane over bifunctional CuO-ZnO/Al2O3 catalyst. Int J Hydrogen Energy 2015;40(40):14052–7.
[21] Pechenkin AA, Badmaev SD, Belyaev vd, Sobyanin VA. Performance of bifunctional CuO–CeO2/Al2O3 catalyst in dimethoxymethane steam reforming to hydrogen-rich gas for fuel cell feeding. Appl Catal B Environ 2015;166–167:535–43.
[22] Pechenkin AA, Badmaev SD, Belyaev v d, Paukshtis EA, Stonkus OA, Sobyanin VA. Steam reforming of dimethoxymethane, methanol and dimethyl ether on CuO–ZnO/Al2O3 catalyst. Kinet Catal 2017;58(5):577–84.
[23] Kakoulaki G, Kougias I, Taylor N, Dolci F, Moya J, Jäger-Waldau A. Green hydrogen in Europe – a regional assessment: substituting existing production with electrolysis powered by renewables. Energy Convers Manag 2021;228:113649.
[24] Yu M, Wang K, Vredenburg H. Insights into low-carbon hydrogen production methods: green, blue and aqua hydrogen. Int J Hydrogen Energy 2021;46(41):21261–73.
[25] Armijo J, Philibert C. Flexible production of green hydrogen and ammonia from variable solar and wind energy: case study of Chile and Argentina. Int J Hydrogen Energy 2020;45(3):1541–58.
[26] Altenburg T, Kantel A, German Institute of Development and Sustainability gGmbH, Bonn. Green hydrogen in Namibia. Opportunities and risks; 2024.
[27] Khan MA, Al-Attas T, Roy S, Rahman MM, Ghaffour N, Thangadurai V, et al. Seawater electrolysis for hydrogen production: a solution looking for a problem? Energy Environ Sci 2021;14(9):4831–9.
[28] Panagopoulos A, Haralambous K-J, Loizidou M. Desalination brine disposal methods and treatment technologies - a review. Sci Total Environ 2019;693:133545.
[29] Keith DW, Holmes G, St, Angelo D, Heidel K. A process for capturing CO2 from the atmosphere. Joule 2018;2(8):1573–94.
[30] Erans M, Sanz-Pérez ES, Hanak DP, Clulow Z, Reiner DM, Mutch GA. Direct air capture: process technology, techno-economic and socio-political challenges. Energy Environ Sci 2022;15(4):1360–405.
[31] Fasihi M, Efimova O, Breyer C. Techno-economic assessment of CO2 direct air capture plants. J Clean Prod 2019;224:957–80.
[32] McQueen N, Gomes KV, McCormick C, Blumanthal K, Pisciotta M, Wilcox J. A review of direct air capture (DAC): scaling up commercial technologies and innovating for the future. Prog Energy 2021;3(3):32001.
[33] Bisotti F, Hoff KA, Mathisen A, Hovland J. Direct air capture (DAC) deployment: a review of the industrial deployment. Chem Eng Sci 2024;283:119416.
[34] Bowker M. Methanol synthesis from CO2 hydrogenation. ChemCatChem 2019;11(17):4238–46.
[35] Cordero-Lanzac T, Ramirez A, Navajas A, Gevers L, Brunialti S, Gandía LM, et al. A techno-economic and life cycle assessment for the production of green methanol from CO2: catalyst and process bottlenecks. J Energy Chem 2022;68:255–66.
[36] Fu Y, Shen J. Selective oxidation of methanol to dimethoxymethane under mild conditions over V2O5/TiO2 with enhanced surface acidity. Chem Commun (Cambridge, England) 2007;(21):2172–4.
[37] Thavornprasert K, Capron M, Jalowiecki-Duhamel L, Dumeignil F. One-pot 1,1-dimethoxymethane synthesis from methanol: a promising pathway over bifunctional catalysts. Catal Sci Technol 2016;6(4):958–70.
[38] Yu H, Zeng K, Fu X, Zhang Y, Peng F, Wang H, et al. RuO 2 · x H 2 O supported on carbon nanotubes as a highly active catalyst for methanol oxidation. J Phys Chem C 2008;112(31):11875–80.
[39] Yuan Y, Shido T, Iwasawa Y. The new catalytic property of supported rhenium oxides for selective oxidation of methanol to methylal. Chem Commun (Cambridge, England) 2000;(15):1421–2.
[40] Liu H, Iglesia E. Selective one-step synthesis of dimethoxymethane via methanol or dimethyl ether oxidation on H 3+ n V n Mo 12- n PO 40 keggin structures. J Phys Chem B 2003;107(39):10840–7.
[41] Sun R, Delidovich I, Palkovits R. Dimethoxymethane as a cleaner synthetic fuel: synthetic methods, catalysts, and reaction mechanism. ACS Catal 2019;9(2):1298–318.
[42] Ren J, Xin F, Xu Y. A review on direct synthesis of dimethoxymethane. Chin J Chem Eng 2022;50:43–55.
[43] Adam R, Cabrero-Antonino JR. Sustainable production of dialkoxymethane ethers and related acetals using CO 2 H 2 and alcohols or diols. ChemCatChem 2024;16(21).
[44] Gierlich CH, Beydoun K, Klankermayer J, Palkovits R. Challenges and opportunities in the production of oxymethylene dimethylether. Chem Ing Tech 2020;92(1–2):116–24.
[45] Wu L, Li B, Zhao C. Direct synthesis of hydrogen and dimethoxylmethane from methanol on copper/silica catalysts with optimal Cu +/Cu 0 sites. ChemCatChem 2018;10(5):1140–7.
[46] Thenert K, Beydoun K, Wiesenthal J, Leitner W, Klankermayer J. Ruthenium-catalyzed synthesis of dialkoxymethane ethers utilizing carbon dioxide and molecular hydrogen. Angew Chem Int Ed 2016;55(40):12266–9.
[47] Schemme S, Breuer JL, Köller M, Meschede S, Walman F, Samsun RC, et al. H2-based synthetic fuels: a techno-economic comparison of alcohol, ether and hydrocarbon production. Int J Hydrogen Energy 2020;45(8):5395–414.
[48] MITSUBISHI. LCO_2 carrier. Available from: https://solutions.mhi.com/ccus/lco2-carrier/. [Accessed 11 June 2025].
[49] Riviera. IMO will change flammable liquid training guidance. Available from: https://www.rivieramm.com/news-content-hub/news-content-hub/imo-will-change-flammable-liquid-training-guidance-38595?.
[50] Lumpp B, Rothe D, Pastötter C, Lämmermann R, Jacob E. Oxymethylene ethers as diesel fuel additives of the future. MTZ Worldw 2011;72(3):34–8.
[51] Liu J, Wang L, Wang P, Sun P, Liu H, Meng Z, et al. An overview of polyoxymethylene dimethyl ethers as alternative fuel for compression ignition engines. Fuel 2022;318:123582.
[52] Pitsch H, Goeb D, Cai L, Willems W. Potential of oxymethylene ethers as renewable diesel substitute. Prog Energy Combust Sci 2024;104:101173.
[53] Sazali N. Emerging technologies by hydrogen: a review. Int J Hydrogen Energy 2020;45(38):18753–71.
[54] Fayaz H, Saidur R, Razali N, Anuar FS, Saleman AR, Islam MR. An overview of hydrogen as a vehicle fuel. Renew Sustain Energy Rev 2012;16(8):5511–28.
[55] Rahim Malik F, Yuan H-B, Moran JC, Tippayawong N. Overview of hydrogen production technologies for fuel cell utilization. Eng Sci Technol Int J 2023;43:101452.
[56] Badmaev SD, Belyaev VD, Snytnikov PV, Sobyanin VA. Electrochemical separation of pure hydrogen from the products of steam reforming of methanol, dimethoxymethane and dimethyl ether. Int J Hydrogen Energy 2025;150:150180.
[57] Badmaev SD, Sobyanin VA. Steam reforming of dimethoxymethane to hydrogen-rich gas over bifunctional CuO-ZnO/Al2O3 catalyst-coated FeCrAl wire mesh. Catal Today 2020;348:9–14.
[58] Semelsberger TA, Ott KC, Borup RL, Greene HL. Role of acidity on the hydrolysis of dimethyl ether (DME) to methanol. Appl Catal B Environ 2005;61(3–4):281–7.
[59] Zhang X, Kirilin AV, Rozeveld S, Kang JH, Pollefeyt G, Yancey DF, et al. Support effect and surface reconstruction in in 2 O 3/m- ZrO 2 catalyzed CO 2 hydrogenation. ACS Catal 2022;12(7):3868–80.
[60] Cui W-G, Zhang Q, Zhou L, Wei Z-C, Yu L, Dai J-J, et al. Hybrid MOF template-directed construction of hollow-structured In2 O3 ZrO2 heterostructure for enhancing hydrogenation of CO2 to methanol. Small 2023;19(1):e2204914.
[61] Baranowski CJ, Bahmanpour AM, Kröcher O. Catalytic synthesis of polyoxymethylene dimethyl ethers (OME): a review. Appl Catal B Environ 2017;217:407–20.